Regulation of Proliferation-Survival Decisions during Tumor Cell Hypoxia

CORNELIUS SCHMALTZ,[1,2]† PATRICIA HARRIGAN HARDENBERGH,[1,2,3]‡
AUDREY WELLS,[1] AND DAVID E. FISHER[1,2,4]*

*Dana-Farber Cancer Institute,[1] Children's Hospital,[4] Joint Center for
Radiation Therapy,[3] and Harvard Medical School,[2]
Boston, Massachusetts 02115*

Hypoxia may influence tumor biology in paradoxically opposing ways: it is lethal as a direct stress trigger, yet hypoxic zones in solid tumors harbor viable cells which are particularly resistant to treatment and contribute importantly to disease relapse. To examine mechanisms underlying growth-survival decisions during hypoxia, we have compared genetically related transformed and untransformed fibroblast cells in vitro for proliferation, survival, clonogenicity, cell cycle, and p53 expression. Hypoxia induces G_0/G_1 arrest in primary fibroblasts but triggers apoptosis in oncogene-transformed derivatives. Unexpectedly, the mechanism of apoptosis is seen to require accumulated acidosis and is rescued by enhanced buffering. The direct effect of hypoxia under nonacidotic conditions is unique to transformed cells in that they override the hypoxic G_0/G_1 arrest of primary cells. Moreover, when uncoupled from acidosis, hypoxia enhances tumor cell viability and clonogenicity relative to normoxia. p53 is correspondingly upregulated in response to hypoxia-induced acidosis but downregulated during hypoxia without acidosis. Hypoxia may thus produce both treatment resistance and a growth advantage. Given strong evidence that hypoxic regions in solid tumors are often nonacidotic (G. Helmlinger, F. Yuan, M. Dellian, and R. K. Jain, Nat. Med. 3:177–182, 1997), this behavior may influence relapse and implicates such cells as potentially important therapeutic targets.

One of the hallmarks of cancer treatment is the frequent ability to achieve remission which is inevitably followed by relapse. This behavior is typical of nearly every common human cancer and strongly implies that within an individual patient, tumor cells are not homogeneous in their treatment sensitivities. Numerous mechanisms of resistance have been demonstrated, including the presence of drug resistance transporters, mutated or amplified drug targets, altered drug metabolism, altered DNA repair, overexpression of antiapoptotic genes, inactivity of proapoptotic gene products, and noncell autonomous features of tumor growth in vivo, such as the presence of hypoxia in solid tumors (36). Disordered tumor cell perfusion and resulting hypoxia may be particularly important as features conferring tumor inhomogeneity which may contribute to relapse following tumor shrinkage during therapy. Studies of solid tumor cells have suggested that through induction of apoptosis, hypoxia may select for cells with defective apoptotic regulators such as p53 (19). Through understanding the behavior of such hypoxic tumor cells, strategies which better target this potentially dangerous cancer cell population may be devised.

Hypoxic regions are a common feature of solid tumors (32, 37, 54). The primary features of tumor physiology that lead to hypoxia are limited arteriolar supply and arteriolar deoxygenation (8), relatively low vascular density and disorderly vascular architecture (46), oxygen consumption rates that are out of balance with oxygen supply (47), and an unstable blood supply (29). Cells in hypoxic regions constitute a clinically relevant problem, because they are more resistant than their normoxic counterparts to the effects of radiotherapy and many conventional chemotherapeutic agents (16, 53; for a review, see reference 52) and are thought to contribute importantly to disease relapse. The presence of hypoxia may also be involved in the development of a more aggressive phenotype and contribute to metastasis (6, 45).

Despite the treatment resistance which it may confer, hypoxia is also directly toxic to most cell types. In recent years, hypoxia has been shown to produce a G_0/G_1 checkpoint as well as accumulation of p53, although p53 seems not to be required for the cell cycle arrest (20). Hypoxia may also induce apoptosis in tumor cells (49, 58) and has recently been implicated in the selection for p53-deficient tumor cells with a diminished apoptotic potential in central (hypoxic) areas of solid tumors (19).

Thus, two seemingly opposing effects of hypoxia exist, one protective and the other directly toxic. The protective effect of hypoxia in conjunction with radiation has long been explored and has led to the development of a model according to which DNA radicals generated by radiation react with oxygen to form organic peroxides that "fix" the radiation damage (oxygen fixation hypothesis). To achieve the same biological effect in hypoxic tissues as in aerated tissues, a 2.5- to 3-fold higher dose of radiation has to be used, a factor known as the oxygen enhancement ratio (22). In contrast to the protective effects of hypoxia, less is known about underlying mechanisms through which hypoxia under certain conditions is toxic or growth suppressive. Potential triggers of tumor cell apoptosis include DNA damage (e.g., radiation or chemotherapy) as well as alternative stress-inducing, but non- DNA-damaging, treatments such as growth factor starvation (11), microtubule poisoning (55, 57), heat (10, 51), and hypoxia (49, 58).

* Corresponding author. Mailing address: Department of Pediatric Oncology, Dana Farber Cancer Institute, 44 Binney St., Boston, MA 02115. Phone: (617) 632-4916. Fax: (617) 632-2085. E-mail: david_fisher @dfci.harvard.edu.

† Present address: University Children's Hospital, 79106 Freiburg, Germany.

‡ Present address: Department of Radiation Oncology, Duke University Medical School, Durham, NC 27710.

p53 protein, a central regulator in tumor cell apoptosis, has been shown to accumulate following exposure of cultured cells to hypoxia (20), displaying increased DNA binding and transactivation capacity. The mechanism for p53 induction by hypoxia remains unclear. The transcription factor hypoxia-inducible factor acts as a global transcriptional regulator for a number of hypoxia-induced genes, including those for erythropoietin, vascular endothelial growth factor, and many of the glycolytic enzymes (reviewed in reference 13). The cellular oxygen-sensing system that in turn regulates hypoxia-inducible factor remains to be elucidated, but preliminary evidence suggests the involvement of a hemoprotein (reviewed in reference 21). A clear mechanistic link between hypoxia and initiation of the apoptotic pathway, however, has not yet been established.

To examine the mechanism underlying apoptosis in hypoxic tumor cells, we have compared genetically related transformed and untransformed rodent fibroblast cells in vitro for cell cycle, proliferation, survival, clonogenicity, and p53 expression under conditions of hypoxia. Hypoxia induced a G_0/G_1 checkpoint in primary fibroblasts but induced apoptotic death in their oncogene-transformed derivative lines. However, the mechanism of apoptosis was seen to require metabolic acidosis. The direct effect of hypoxia under nonacidotic conditions was unique to transformed cells in that they override the hypoxic G_0/G_1 checkpoint seen in primary cells. Moreover, when uncoupled from acidosis, hypoxia enhanced tumor cell viability and clonogenicity relative to normoxia. p53 was correspondingly upregulated in response to hypoxia-induced acidosis but was greatly downregulated under conditions of hypoxia without acidosis.

MATERIALS AND METHODS

Cell culture. Except for the experiment with the results shown in Fig. 5b, E1a/Ras-transformed $p53^{+/+}$ and $p53^{-/-}$ mouse embryo fibroblasts (MEF) (34) were maintained in Dulbecco's modified Eagle's medium containing 4.5 g of glucose per liter and no HEPES buffer (Mediatech, Herndon, Va.) and supplemented with 10% newborn calf serum and 10% fetal bovine serum (BioWhittaker, Walkersville, Md.) and 292 µg of L-glutamine per ml, 100 U of penicillin sodium per ml, and 100 µg of streptomycin sulfate per ml (Gibco BRL, Grand Island, N.Y.). Early-passage (passage 1 to 4) untransformed rat embryo fibroblasts (REF) (primary REF obtained from BioWhittaker) and Myc/Ras-transformed REF, derived from transfection of primary REF with c-Myc and Ras plasmids followed by clonal expansion of foci, were maintained in minimum essential medium (Mediatech) supplemented as described above. For the experiment with the results shown in Fig. 5b, Dulbecco's modified Eagle's medium with and without 25 mM HEPES buffer, normalized for osmolarity (Gibco BRL, Gaithersburg, Md.), was used. All cells were maintained in a humidified atmosphere of 5% CO_2 at 37°C.

Hypoxia. For all experiments involving hypoxia (and the respective normoxic controls), cells were grown on 60-mm-diameter Permanox tissue culture dishes, which are greater than 100-fold more O_2 permeable than other plastics (Nunc, Naperville, Ill.), circumventing the slow release of oxygen from polystyrene (31). In a modification of Koch's thin-film culturing technique (30), only 1.5 to 1.7 ml of medium was used to facilitate rapid deoxygenation of the medium. For the experiment of Fig. 5c and d requiring additional medium, medium was degassed in flat glass plates in the hypoxic tissue culture hood for at least 24 h prior to being added to the plates in the anaerobic chamber device. Cells were seeded at a given density and were always permitted to attach for 16 to 20 h in atmospheric oxygen before exposure to hypoxia.

Hypoxia was achieved in two ways. For the first method, tissue culture dishes were sealed in aluminum hypoxia chambers which were subjected to eight gas exchanges with 95% N_2–5% CO_2 (Medical-Technical Gases Inc., Medford, Mass.) (certified to contain less than 10 ppm O_2) and subsequently kept at 37°C (50). Controls which underwent identical gas exchanges but were then filled with air showed no differences in number or viability from cells grown under normal conditions. For the second method of producing hypoxia, tissue culture dishes were placed in a Bactron Anaerobic/Environmental Chamber (Sheldon Manufacturing Inc., Cornelius, Oreg.) with a self-contained incubator unit that uses a 90% N_2–5% H_2–5% CO_2-injected atmosphere and a palladium catalyst. The oxygen tension in the chamber, as measured by an oxygen analyzer (Illinois Instruments Inc., Ingleside, Ill.) was <40 ppm.

DAPI staining and fluorescence microscopy. Cells and cell fragments were cytospun, fixed with methanol-acetic acid (3:1) for 30 min, stained with a 0.01-mg/ml solution of 4′,6-diamidino-2-phenylindole (DAPI) (Sigma, St. Louis, Mo.) for 15 min, and subsequently destained with methanol for 1 to 3 h. Fluorescence

microscopy was with an Axioskop (Carl Zeiss Inc., Thornwood, N.Y.). Photomicrographs were obtained at a magnification of ×60.

DNA ladders, Annexin V staining, and flow cytometry. Floating and trypsinized cells were harvested, pooled, and rinsed twice in cold phosphate-buffered saline (PBS). Staining of exposed phosphatidylserine was performed according to the instructions provided in the TACS Annexin V-FITC Kit (Trevigen, Inc., Gaithersburg, Md.). Fluorometric quantitation of Annexin V conjugates was performed with CellQuest Software on a FACScan flow cytometer (Becton Dickinson). Genomic DNA was analyzed for ladder formation according to the method of Herrmann et al. (24).

Viability and clonogenic assays. Floating and trypsinized adherent cells were pooled, resuspended in PBS, and mixed 1:1 with 0.4% trypan blue (Gibco BRL). Tissue culture dishes for clonogenic assays were prepared with feeder layers of E1a/Ras-transformed MEF, plated at a density of 2×10^6/60-mm-diameter dish, and irradiated with 2,500 cGy the next day. On the following day, previously oxic or hypoxic cells (immediately following 30 h of hypoxia or control incubation) were seeded at 500 to 5,000 cells/plate. After 7 days in a humidified incubator containing 5% CO_2 at 37°C, plates were fixed and stained with a solution of 0.1% crystal violet in 90% ethanol, and colonies containing more than 50 cells were scored. The plating efficiency (PE) was calculated as the number of colonies on one plate divided by the number of cells seeded on that plate. The surviving fraction is the PE of treated cells divided by the PE of the untreated controls.

Cell cycle analysis. Propidium iodide (PI) was used to determine the DNA content of fixed cells. Cells were harvested and fixed for at least 30 min in 50% ethanol immediately after hypoxic treatment and then incubated for 30 min in a solution of 2.5 µg of PI per ml and 50 µg of RNase A per ml. Flow cytometry was carried out on a FACScan (Becton Dickinson) with CellQuest Software. The data were subsequently analyzed with ModFitLT V1.01 for cell cycle determination. For Fig. 6c, the cells were pulse-labeled by the addition of 1.7 µl of bromodeoxyuridine (BrdU) (previously degassed) to the 1.7 ml of culture medium (final concentration, 10 µM BrdU) during the last 30 min of their hypoxic incubation. Cells were harvested, fixed, and stained as described previously (9). Briefly, cells fixed in 50% ethanol were treated with RNase A, followed by incubation in 0.1 M HCl–0.5% Triton X-100 and DNA denaturation at 95°C for 10 min. A fluorescein isothiocyanate-conjugated monoclonal anti-BrdU antibody (Pharmingen, San Diego, Calif.) was employed to detect BrdU uptake, cells were counterstained with PI for DNA content, and flow cytometry with CellQuest Software was carried out on a FACScan.

pH measurement. Immediately after hypoxic exposure, the medium from three identically treated plates was pooled, and the pH was measured with a combination electrode ("3-in-1-combination"; Corning, Corning, N.Y.) and an electronic pH meter (pH meter 320; Corning). Measurements were made within 1 min after termination of hypoxic treatment.

Irradiation. Cells growing on tissue culture plates were irradiated from a ^{137}Cs source (Gammacell 40; Atomic Energy of Canada Limited) at a rate of 1 Gy/min.

p53 immunoblot. Cells were harvested immediately after treatment (hypoxic cells were harvested under hypoxic conditions to avoid reoxygenation), lysed in 3% sodium dodecyl sulfate–2% glycerol, and denatured for 5 min at 96°C. Lysates of 600,000 cells per well were separated by 8% polyacrylamide gel electrophoresis and transferred onto a nitrocellulose filter (Schleicher & Schuell). Protein was detected by using a monoclonal p53 antibody (Pab 421; Calbiochem) and a horseradish peroxidase-coupled secondary antibody (Cappel) and then visualized by enhanced chemiluminescence (100 mM Tris [pH 8.5], 2.5 mM luminol, 400 µM coumaric acid, 5.3 mM H_2O_2).

In vitro cleavage of PARP by cell extracts. Cytosolic extracts were isolated from E1a/Ras-transformed MEF immediately after the hypoxic or normoxic incubation for 20 h of cells seeded at 2×10^6 cells/60-mm-diameter plate and prepared essentially as previously described (40). Adherent and floating cells were pooled, washed in PBS, lysed in buffer A (20 mM HEPES [pH 7.4], 10 mM KCl, 15 mM $MgCl_2$, 1 mM EDTA, 1 mM EGTA, 3 mM dithiothreitol, 4 mM Pefabloc, 5 µg of pepstatin A per ml, 10 µg of leupeptin per ml, 10 µg of aprotinin per ml), flash frozen and thawed once, and then centrifuged at $100,000 \times g$ for 1 h. Fifty nanograms of a His$_6$-tagged N-terminal poly(ADP)-ribose polymerase (PARP) fragment, which spans the specific cysteine protease cleavage site (the plasmid was generously provided by John Collier, Harvard Medical School) was added to 10 µl of $100,000 \times g$ supernatant and incubated at 37°C for 15 min. Samples were resolved on sodium dodecyl sulfate–12% polyacrylamide minigels and transferred to nitrocellulose. Protein was detected with the C2-10 anti-PARP mouse monoclonal antibody (a gift of Guy Poirier, Université Laval, Quebec, Canada) and a peroxidase-conjugated secondary antibody (Cappel) and visualized by enhanced chemiluminescence.

RESULTS

Hypoxia differentially triggers cell cycle arrest versus apoptosis, depending on oncogenic transformation. Hypoxia (<40 ppm O_2) significantly impaired proliferation of early-passage (before passage 4) primary untransformed REF in culture (Fig. 1a). The cell count per plate remained virtually constant 24 and 48 h after exposure to hypoxia, whereas cells on nor-
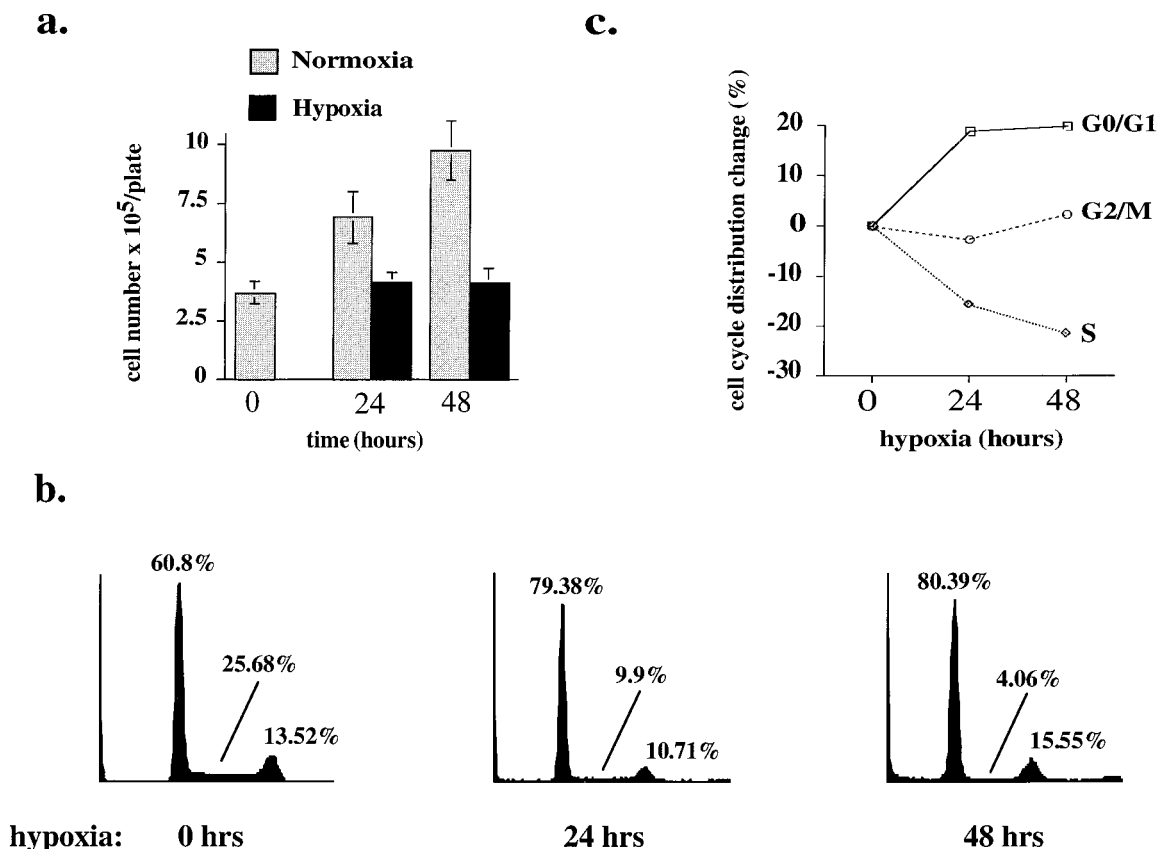
a.

c.

b.

hypoxia: **0 hrs**   **24 hrs**   **48 hrs**

FIG. 1. (a) Hypoxia-induced growth arrest in untransformed REF. Cells were plated at a density of 2×10^5/60-mm-diameter dish, and exposure to hypoxia was started approximately 16 h later (time zero). At 0, 24, and 48 h, cells were harvested and the number of viable (trypan blue-excluding) cells per 60-mm-diameter dish was counted. Results of experiments in triplicate are expressed as means ± standard deviations. (b) Hypoxia-induced G_1-arrest in untransformed REF. The DNA content of fixed and PI-stained cells from the same experiment described for panel a was measured by flow cytometry, and cell cycle analysis was performed. Percentages of cells in each phase of the cell cycle are given for each diagram. (c) Absolute changes in distribution of cells in the cell cycle. Percentages immediately before exposure to hypoxia are taken as the starting point (0); absolute increases and decreases in the percentages of cells in G_1/G_0, S, and G_2/M after 24 and 48 h are plotted. All studies are representative of at least three independent experiments.

moxic control plates proliferated, increasing threefold within 48 h. Both hypoxic and normoxic cells remained virtually 100% viable by trypan blue exclusion. Cell cycle analysis by flow cytometric measurement of DNA content revealed that hypoxic cells arrested predominantly in G_0/G_1, with a concomitant decrease in S phase cells (Fig. 1b and c). The percentage of cells in S phase decreased from 25% in normoxic controls to 4% after 48 h of hypoxia. The G_0/G_1 fraction increased from 60.8 to 80.4%, with a stable percentage (13.5 to 15.5%) of cells in G_2/M. These observations suggest the activation of a G_0/G_1 checkpoint by hypoxia. Confluence did not contribute to this arrest, as the cell number over the study period remained well below confluence (and as evidenced by the proliferation of normoxic cells).

In contrast to primary fibroblasts, Myc/Ras-transformed REF (derived from the same primary cells) exhibited apoptotic death following hypoxia, whereas primary REF remained viable under identical conditions (Fig. 2a and c). This comparison is based on stable, phenotypically transformed derivative lines and early-passage primary fibroblasts (rather than vector-transformed primary cells). Analysis of p53 wild-type and null E1a/Ras-transformed MEF (Fig. 2b and d) also revealed apoptosis in response to hypoxia rather than cell cycle arrest. Apoptosis was quantitated by flow cytometry and Annexin V staining, which assays flippage of phosphatidylserine to the outer cyto-

plasmic membrane (12). As shown in histograms of these analyses (Fig. 2c and d), essentially the entire population of hypoxic Myc/Ras-transformed REF and p53$^{+/+}$ E1A/Ras-transformed MEF underwent apoptosis, in contrast to minimal changes from baseline values in hypoxic REF (Fig. 2c) or normoxic control Myc/Ras-transformed REF (data not shown). Consistent with Annexin V positivity representing an earlier phase in the death pathway than loss of membrane integrity, Annexin V staining identified apoptotic cells at earlier times of hypoxia than trypan blue staining. In agreement with the results of Graeber et al. (19), the presence of p53 modulated the response to hypoxia. p53-deficient E1a/Ras-transformed MEF were somewhat resistant (or delayed) in the apoptotic response, although with longer hypoxia extensive death was seen in this population as well (Fig. 2b and d) (some of this may be nonapoptotic death, based on morphology [data not shown]).

Further evidence for apoptosis in hypoxic p53 wild-type tumor cells (in addition to phosphatidylserine flippage) included endonucleolytic DNA cleavage (laddering), which was apparent in the hypoxic cells (Fig. 3a). DAPI staining revealed shrinkage, nuclear condensation, and fragmentation, the morphological hallmarks of apoptosis (Fig. 3b). Cleavage of a PARP fragment in an in vitro assay of cytosolic extracts from these cells (Fig. 3c) revealed activation of caspases which function in the execution of apoptosis (28, 33). Thus, in agreement
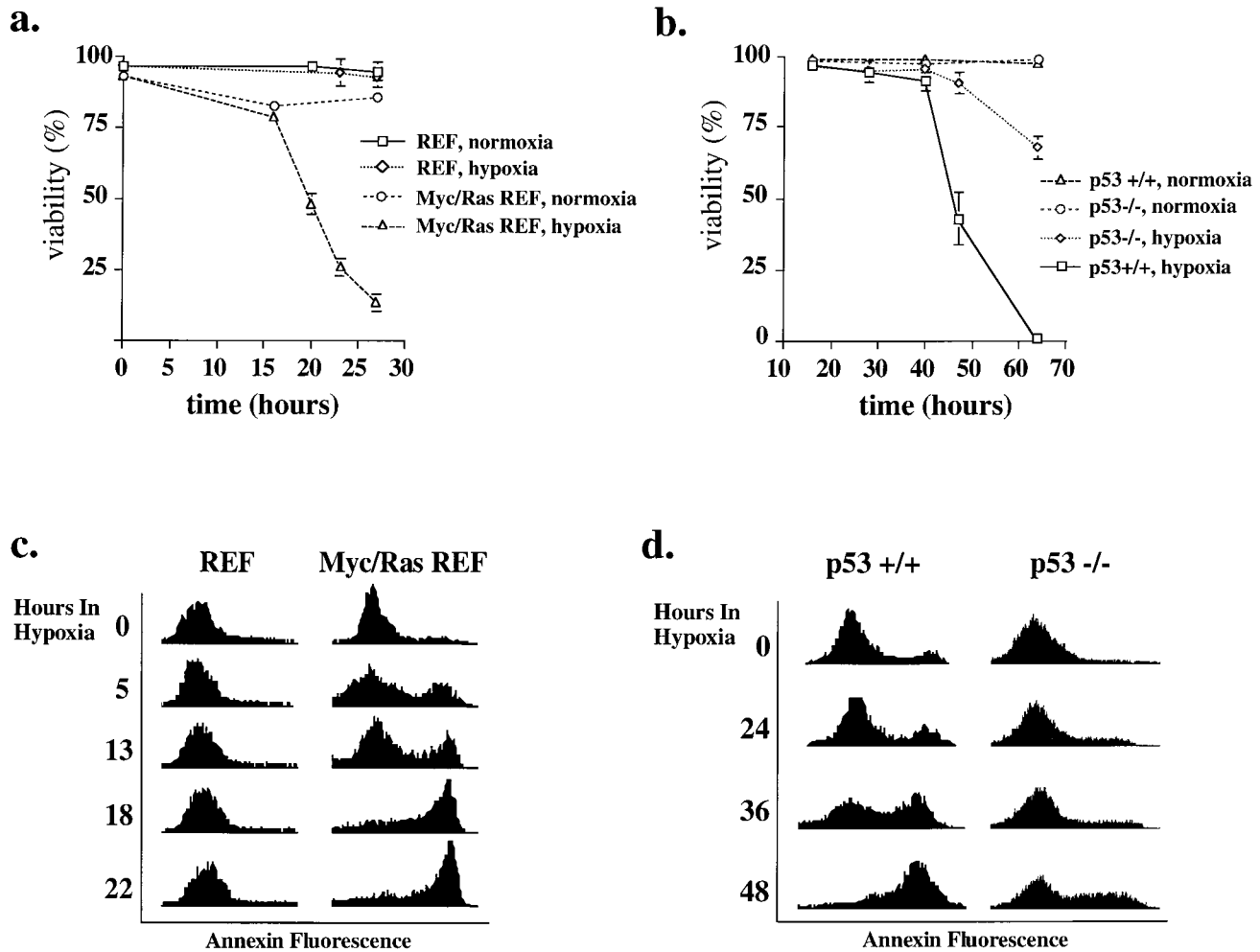
a.

b.

c.

d.

FIG. 2. Viability of cells under hypoxic conditions. (a and b) Cells plated at a density of 5×10^5 cells/60-mm-diameter dish were kept in a hypoxic environment for different time periods, and their viability was quantitated by exclusion of trypan blue. Values for normoxic control plates were measured at the same time points; the viability of these cells reflects a small degree of background apoptosis but does not change over the course of the experiment. Results of experiments in triplicate are expressed as means $\pm$ standard deviations. (a) REF and c-Myc/Ras-transformed REF. (b) E1a/Ras-transformed MEF ($p53^{+/+}$ and $p53^{-/-}$). (c and d) Phosphatidylserine exposure as a quantitative measure of apoptosis. Untransformed REF or Myc/Ras-transformed REF (c) and E1a/Ras-transformed MEF ($p53^{+/+}$ or $p53^{-/-}$) (d) were plated at 5×10^5 cells/60-mm-diameter dish and rendered hypoxic for the time periods indicated. Flow cytometry for Annexin V staining (indicating phosphatidylserine flippage) produced histograms which demonstrate apoptotic death in hypoxic transformed cells (fluorescence intensity for Annexin V is plotted on the x axis, and cell number is plotted on the y axis). Phosphatidylserine flippage precedes trypan blue permeability (a and b).

with prior analyses of p53 wild-type tumor cells (19), hypoxic exposure resulted in profound apoptotic death.

Density dependence of hypoxia-triggered apoptosis. To investigate the mechanism underlying hypoxia-induced apoptosis, this process was examined at different cell densities. Unexpectedly, at lower densities, Myc/Ras-transformed REF were resistant to the identical hypoxic exposure (Fig. 4a). At 5×10^5 cells/60-mm-diameter dish, the transformed cell line displayed profound cell death after 17 h of hypoxia, whereas at a density of 1×10^5 cells/60-mm-diameter dish, viability was virtually identical to that of normoxic cultures at all densities. Of note, the range of cell densities in these experiments is far from confluence, which is reached at densities of $>4 \times 10^6$ cells/60-mm-diameter dish for these cell lines. A dose effect appeared to operate, in which the toxicity of hypoxia was linearly dependent upon cell density. This same density effect was also seen in E1a/Ras-transformed MEF (Fig. 4b). As shown in Fig. 2c and d and 3, the death observed at higher density is apoptosis. Again, the $p53^{-/-}$ cells appeared to be relatively resistant. In contrast to the density-dependent responses of trans-

formed fibroblasts to hypoxia, untransformed fibroblasts (REF) underwent G_0/G_1 cell cycle arrest regardless of cell density (Fig. 1 and data not shown).

Role of pH in hypoxia-triggered apoptosis. To examine the mechanism through which density influences hypoxia-triggered apoptosis, we measured the pH of the medium and observed the presence of acidosis, which correlated with cell density and hypoxic exposure (Fig. 5a). For example, the pH was 6.5 for E1a/Ras-transformed MEF after 24 h of hypoxia at high density but reached this pH only after 48 h at intermediate density. Moreover, the more rapid kinetics of death for Myc/Ras-transformed REF (Fig. 2a) also correlated with acidification kinetics. These cells acidify the medium to pH 6.5 after only 24 h (at the intermediate density of 5×10^5 per plate), while E1a/Ras-transformed MEF reach the same degree of acidosis after 48 h (Fig. 5a). This suggested that an indirect metabolic consequence of hypoxia, rather than a direct effect of hypoxia itself, could be triggering the apoptotic pathway. Such mechanisms could include nutrient deprivation (see Discussion) or acidosis.

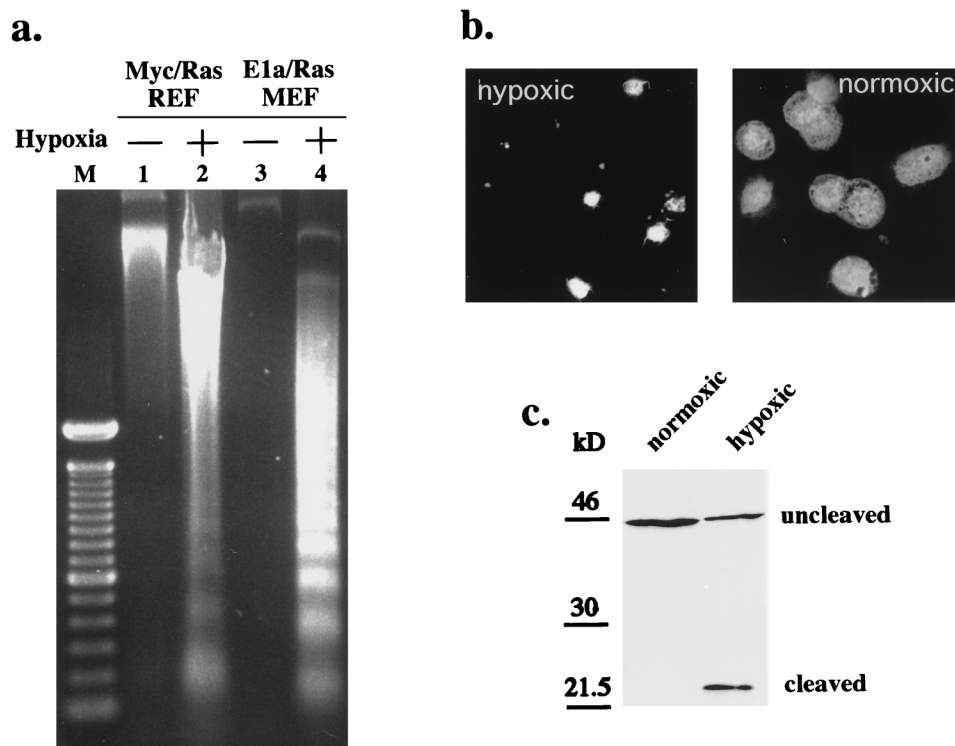To test this hypothesis, acidosis was neutralized in several

a.

b.

c.

FIG. 3. (a) Internucleosomal DNA cleavage as a marker of hypoxia-induced apoptosis. Genomic DNA from normoxic or hypoxic cells (5×10^5 cells/60-mm-diameter plate) was electrophoretically resolved and revealed laddering in hypoxic cells but not in normoxic controls. M, markers. (b) Apoptotic morphology of cells exposed to 48 h of hypoxia at high density. Hypoxic E1a/Ras-transformed MEF (p53$^{+/+}$) were fixed and stained for nuclear morphology with DAPI. Fluorescence microscopy demonstrates nuclear condensation and fragmentation (including apoptotic bodies) in the hypoxic cells compared to oxic controls (identical magnifications and exposures were used). (c) PARP cleavage activity in hypoxia-triggered apoptosis. Equal amounts of cytoplasmic extracts from hypoxic and normoxic E1a/Ras-transformed MEF (p53$^{+/+}$) were incubated with a recombinant N-terminal PARP fragment. Immunoblotting shows PARP cleavage activity in the hypoxic extract but no PARP cleavage activity in equivalent extracts from normoxic cells.

ways. E1a/Ras-transformed MEF (p53$^{+/+}$) at a higher density (2×10^6 cells/60-mm-diameter dish; ~50% confluence) were rendered hypoxic in the presence of either (i) medium modified by the addition of 25 mM HEPES buffer or (ii) a larger volume of previously deoxygenated standard medium. Both of these modifications increased buffering capacity. While control plates with 1.7 ml of medium displayed >80% cell death after 20 h of hypoxia, cells of the same density cultured with 5 ml of deoxygenated medium or with 1.7 ml of the HEPES-containing medium were rescued up to 100 and 80% of the values for their normoxic counterparts, respectively (Fig. 5b and c). Lack of acidification accompanied this rescue; the pH of 5 ml of medium after hypoxia was 7.6, compared to 6.8 for the smaller volume. These experiments demonstrate that augmentation of the buffer capacity ameliorates hypoxia-triggered cell death.

Conversely, we tested whether acidosis alone, under nonhypoxic conditions, is sufficient to trigger apoptosis in cells grown at a low density (10^5/plate). Medium was acidified with HCl down to the pH seen in high-density hypoxic cultures (pH 6.5) or acidified and then reneutralized with NaOH. Both Myc/Ras-transformed REF and E1a/Ras-transformed MEF at low density were exposed to preacidified medium and exhibited massive apoptosis after only 5 h (Fig. 5e). Reneutralized medium rescued this apoptotic death. Taken together, these experiments strongly suggest that metabolic acidosis (a predictable consequence of hypoxia) is the more proximal cause of death, rather than hypoxia per se.

Hypoxia enhances proliferation of transformed cells at low density. The rescue of hypoxia's toxicity by preventing acidosis

permitted the analysis of viability, clonogenicity, and the hypoxic cell cycle checkpoint in these viable, hypoxic cells. E1a/Ras-transformed p53$^{+/+}$ and p53$^{-/-}$ fibroblasts were subjected to 30 h of hypoxia at either low density (1×10^5 cells/60-mm-diameter dish) or ~50% confluence (2×10^6 cells/60-mm-diameter dish) prior to quantitation of cell number and viability as well as colony formation. As seen in Fig. 6a, at ~50% confluence both p53$^{+/+}$ and p53$^{-/-}$ E1a/Ras-transformed MEF populations were sensitive to hypoxia, with the p53$^{+/+}$ cells being completely nonviable. In contrast, identical hypoxic treatment at the lower density resulted in increased cell numbers relative to those for normoxic controls (seeded at the same densities). This increase occurred in either the presence or absence of p53. Since the viability quantitation reflects only one time point, cells treated in this manner were also quantified for colony formation (Fig. 6b). In agreement with the cell number increase, clonogenic assays from low-density hypoxic cell cultures resulted in survival fractions that were approximately 50% higher than those in normoxic controls, again independent of p53 presence or absence. Predictably, the higher-density hypoxic cells lost clonogenicity, with p53$^{-/-}$ cells exhibiting a surviving fraction of only 20%.

To directly measure cell cycle progression and the hypoxia G$_0$/G$_1$ checkpoint, E1a/Ras-transformed cells at a low density were pulsed with BrdU during the last 30 min of 30-h hypoxic incubations. These analyses showed complete absence of the hypoxia checkpoint with a consistent modest increase in the percentage of cells in S phase (32.1% of normoxic cells versus 39.4% of hypoxic cells in S phase) (Fig. 6c).
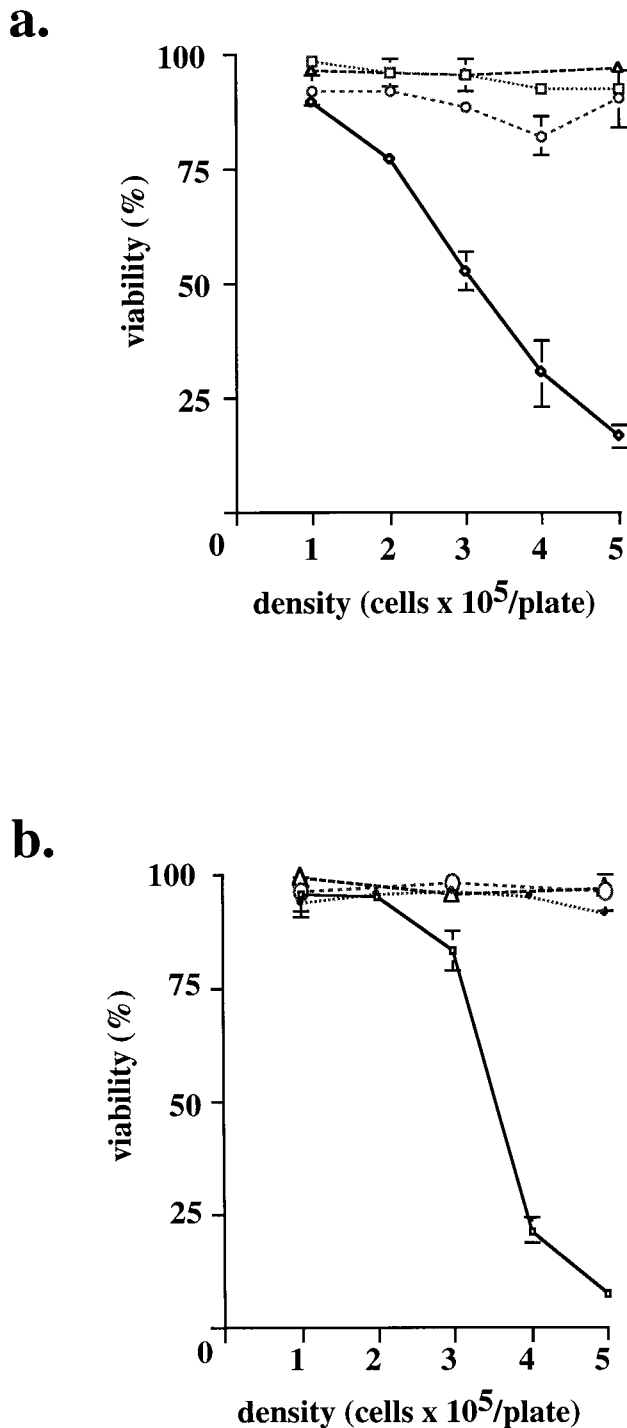
a.

b.

FIG. 4. Viability of transformed cells under hypoxia at different densities. Cells plated at different densities were incubated in a hypoxic environment for a fixed time, and viability was determined by exclusion of trypan blue. Oxic controls of both cell lines were viable at all times of the experiment. Results of experiments in triplicate are expressed as means ± standard deviations. (a) REF and c-Myc/Ras-transformed REF, examined after 24 h of treatment. △, REF, normoxia; □, REF, hypoxia; ○, Myc/Ras REF, normoxia; ◇, Myc/Ras REF, hypoxia. (b) E1a/Ras-transformed MEF (p53$^{+/+}$ and p53$^{-/-}$), examined after 53 h of treatment. ○, p53$^{+/+}$, normoxia; △, p53$^{-/-}$, normoxia; ●, p53$^{-/-}$, hypoxia; □, p53$^{+/+}$, hypoxia.

Hypoxia-induced acidosis upregulates p53 protein, but hypoxia itself downmodulates p53. Given the evidence that p53 responds to and modulates the apoptotic response from hypoxia (19, 20) (Fig. 2b and 4b), it was of interest to examine p53 protein levels under conditions in which the indirect (metabolic) and direct effects of hypoxia could be separated. Immunoblotting was performed with the p53$^{+/+}$ E1a/Ras-transformed MEF, which were rendered hypoxic at either 50% confluence (2×10^6 cells/60-mm-diameter plate) or a lower cell density (1×10^5 cells/60-mm-diameter plate), where hypoxia does not lead to significant acidosis. As seen in Fig. 7 and as reported by others (20), under conditions of hypoxia without neutralization of acidosis, p53 protein levels are modestly upregulated. In contrast, hypoxia without acidosis clearly downregulates p53 protein levels compared to those of oxic cells (Fig. 7). An anti-tubulin control showed no significant differences (Fig. 7), demonstrating the specificity of p53 downregulation by hypoxia. This p53 downregulation correlates with the enhanced proliferation that is observed under low-density, hypoxic conditions (Fig. 6). As a control, ionizing radiation upregulated p53 independent of cell density (Fig. 7).

DISCUSSION

The differential effects of hypoxia on primary and oncogene-transformed cells, causing G$_1$ arrest in the former and apoptosis in the latter, follow the pattern of other triggers of apoptosis or growth arrest, such as ionizing radiation and chemotherapeutic drugs (for a review, see reference 14). The differential effects of these agents on untransformed (normal) and oncogenically transformed (tumor) cells potentially provides a therapeutic window (reviewed in reference 14) that permits the preferential killing of malignant cells in cancer therapy. The mechanism of action for these triggers of p53-mediated apoptosis or arrest has been proposed to involve DNA damage (39). There is, however, growing evidence that signals distinct from DNA damage can also induce p53 and initiate cell death pathways. Hypoxia appears to represent such a non-DNA-damaging signal that elicits these alternative response pathways (G$_0$/G$_1$ arrest versus apoptosis), depending on the cellular context.

Our results suggest, however, that these two responses involve different mechanisms: cell cycle arrest occurs in the absence of measurable acidosis for hypoxic primary fibroblasts, whereas apoptosis of hypoxic transformed fibroblasts appears to require acidosis. In the absence of acidosis, the hypoxic checkpoint in transformed cells appears to be overridden, since S-phase entry is maintained together with increased proliferation, viability, and clonogenicity. In fact, the accumulation of acidosis in transformed cell cultures, but not primary REF, may reflect the presence or absence of a mechanism which modulates cell cycle progression and metabolism more generally.

Role of acidosis. The rapidly decreasing pH of medium under hypoxic conditions suggests the Pasteur effect, the switch from oxidative phosphorylation (Krebs cycle) to glycolysis that occurs under hypoxic conditions. As a consequence of this switch, an increase in the consumption of glucose and the production of lactic acid in order to maintain the same level of energy production is anticipated. If, however, a lower level of energy production is maintained, as may occur in arrested primary cells, glucose consumption and acidosis may not change rapidly. The behavior of different cell lines under hypoxia is thus likely to vary as a function of their metabolic regulation. For example, Shrieve et al. (50) found no difference in the per-cell consumption of glucose and production of lactic acid
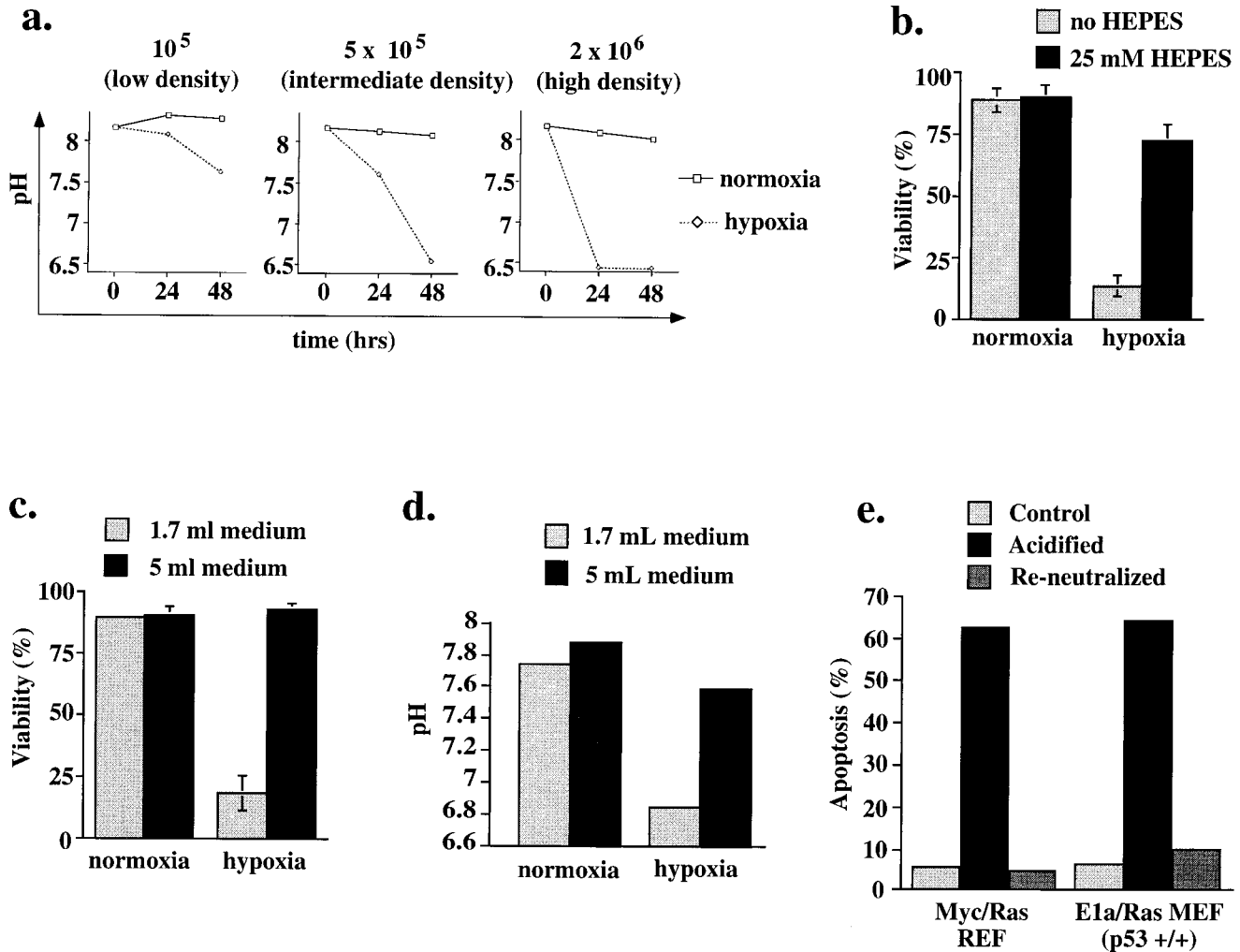
FIG. 5. (a) Decline of medium pH during hypoxia. E1a/Ras-transformed MEF (p53$^{+/+}$) were plated at densities of 1×10^5, 5×10^5, and 2×10^6 cells/60-mm-diameter dish and incubated under hypoxic or normoxic conditions for the time periods indicated. (b and c) Rescue from hypoxia-triggered cell death in E1a/Ras-transformed p53$^{+/+}$ fibroblasts through increased buffer capacity of the medium. Viability was assessed by exclusion of trypan blue. Results of experiments in triplicate are expressed as means ± standard deviations. (b) Additional buffer. Cells were plated at 2×10^6/60-mm-diameter dish and exposed to hypoxia for 22 h in 1.7 ml of either HEPES-free or 25 mM HEPES-containing medium (see Materials and Methods). (c) Increased volume of degassed medium. Cells were plated at 2×10^6/60-mm-diameter dish and exposed to hypoxia for 17 h in the presence of either 1.7 or 5 ml of previously degassed medium. (d) pH of medium correlates with viability. The pH of the medium following incubation under the conditions used for panel c is plotted. (e) Preacidification of medium triggers apoptosis in the absence of hypoxia. Medium was acidified to pH 6.5 (matching the pH of high-density hypoxic p53$^{+/+}$ apoptotic cells) by using HCl or acidified to 6.5 and then reneutralized with NaOH. Myc/Ras-transformed REF or E1a/Ras-transformed MEF (p53$^{+/+}$) were exposed to these media at a low cell density (10^5/60-mm-diameter plate) for 5 h, followed by Annexin V staining and flow cytometric quantitation of apoptosis.

in aerated and hypoxic cultures of EMT6/SF cells, citing evidence that cells adapted to tissue culture and tumor cells may be highly glycolytic, even in air (Warburg effect) (5). In other studies, increases in glucose uptake and lactic acid production have been observed under hypoxic conditions (1, 44). The behavior observed here may thus reflect different energy consumption set points in paired transformed and untransformed cells, and the presence of the hypoxic G_0/G_1 checkpoint may influence this set point.

Scarcity of glucose does not appear to be a death-triggering event under our culture conditions, which include a relatively high level of glucose in the medium. Experiments with glucose addition did not show significant rescue from hypoxic cell death, and medium from cells that were dying in hypoxia could still support cell growth when it was corrected for acidosis (data not shown). Conversely, additional buffer capacity did prevent apoptosis, thereby providing evidence that the trigger

of apoptosis in hypoxic cultures is acid accumulation, likely lactic acidosis. In accordance with this result, low pH and lactate exposure have been shown to inhibit cell proliferation and survival as well as to enhance radiosensitivity (48, for a review, see reference 56).

Acidosis has been associated with cell death in a number of previous systems. DNase II, an endonuclease thought to be important in the internucleosomal cleavage associated with apoptosis, has been shown to be activated at an intracellular pH of below 7 (2, 3), and cell-sorting experiments have strongly correlated intracellular pH and DNA degradation (4, 41). Intracellular pH has been proposed as a downstream effector of apoptosis triggered by diverse agents, such as anti-Fas immunoglobulin M, cycloheximide, UV irradiation (18), growth factor withdrawal (42), etoposide (4), and lovastatin (41). Conversely, inhibition of apoptosis by granulocyte colony-stimulating factor in granulocytes (17), by Bcl-2 in CHO cells (43), or
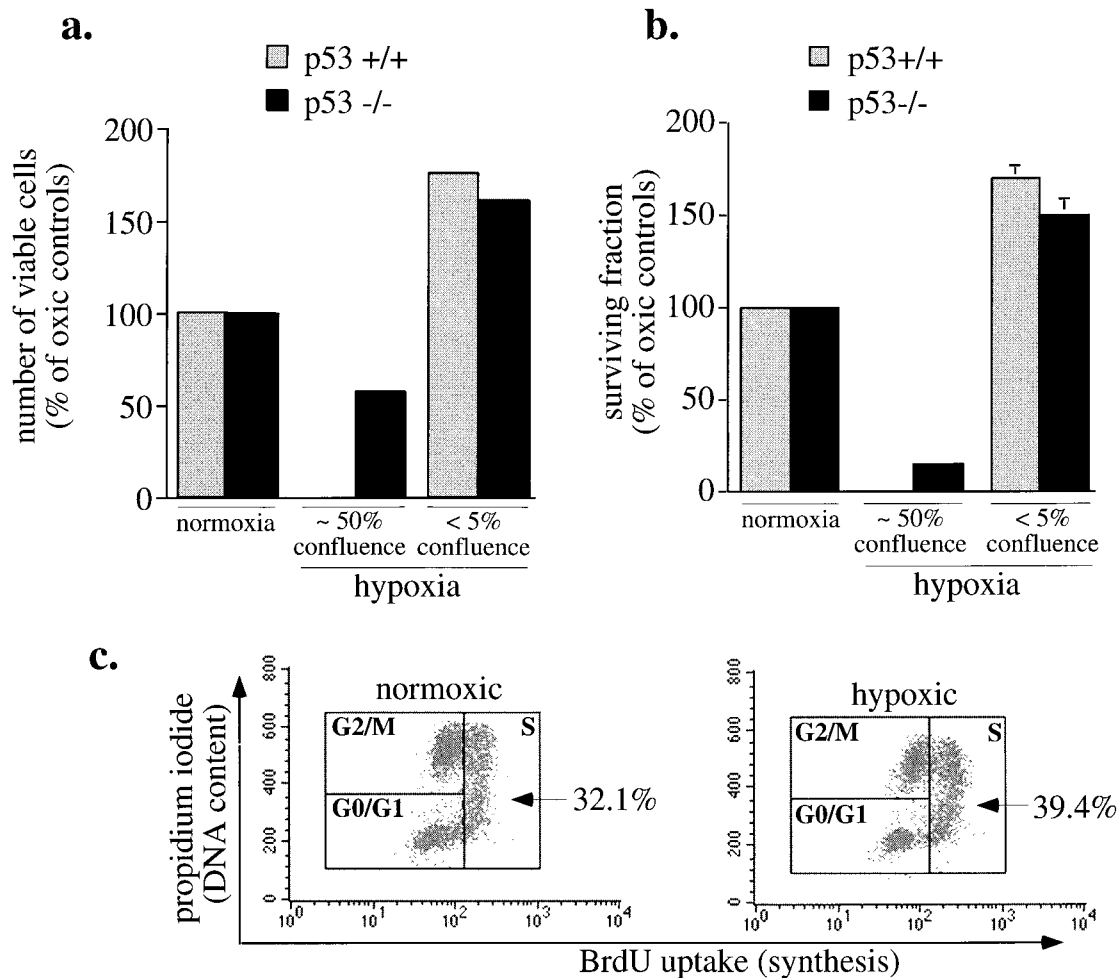
a.

b.

c.

FIG. 6. Effects of hypoxia at various cell densities (a and b) E1a/Ras-transformed MEF (p53$^{+/+}$ and p53$^{-/-}$) were plated at a low density (1 × 10^5/60-mm-diameter dish; <5% confluence) or at a higher density (2 × 10^6/60-mm-diameter dish; ~50% confluence), incubated under hypoxia for 30 h, trypsinized, and assessed for viability by exclusion of trypan blue, (a) or reseeded for clonogenic assays (b). Colonies containing more than 50 cells were scored after 7 days. Results of experiments in triplicate are expressed as means ± standard deviations. (c) Increase in S phase in low-density hypoxic cultures. E1a/Ras-transformed MEF (p53$^{+/+}$) at a low density (10^5/60-mm-diameter dish) were BrdU pulse-labeled for the last 30 min of 30-h hypoxic incubations. S phase was determined by flow cytometry for BrdU uptake and PI staining. Unlike primary fibroblasts, which undergo cell cycle arrest (Fig. 1), transformed fibroblasts fail to arrest and even show a modest but consistent increase in S phase. The results shown are representative of three independent experiments.

by protein phosphatase inhibitors in ML-1 cells (35) prevented intracellular acidification as well as apoptosis. Lovastatin-induced apoptosis could be rescued by stimulation of the Na$^+$/H$^+$ antiport that led to an increase in intracellular pH (41). It will be of interest to examine the intracellular pH, which may correlate with the extracellular acidosis reported here, thereby potentially modulating the apoptosis pathway(s). Acidosis is also potentially a trigger of apoptosis in a number of nonneoplastic clinical circumstances, including the ischemia of myocardial infarction, stroke, and sepsis.

p53 and hypoxia. In addition to the induction of either cell cycle arrest or apoptosis, hypoxia has been demonstrated to induce p53 protein (20). In these studies, hypoxic treatment was found to substantially upregulate p53 protein levels as well as DNA binding and transcriptional activities. However, the G$_0$/G$_1$ arrest produced by hypoxia does not appear to require p53, because the human papillomavirus E6 gene did not abolish this checkpoint (20). In the present studies, p53 was also induced by hypoxia, but in a fashion found to require secondary acidosis. In contrast, p53 levels fell when hypoxia was induced without metabolic acidosis. This ability to uncouple p53

induction from hypoxia by correcting for acidosis also supports the model that acidosis, rather than hypoxia per se, is responsible for the death seen in these cell systems. Our results are consistent with the hypothesis that this form of apoptosis is modulated by the presence or absence of p53 (19). p53 protein levels are regulated largely at the posttranslational stability level, although other modes of regulation may also function. It is unclear whether the p53 downregulation seen here represents a novel p53 turnover mechanism or involves modulation of the same pathway that regulates p53 levels following irradiation or hypoxia with acidosis.

The downregulation of p53 in low-density hypoxic cells also correlates with enhanced S-phase entry in transformed fibroblasts. This observation suggests that background oxidative stress may lead to p53 activation and trigger the p53-dependent G$_1$/S checkpoint under conditions of atmospheric oxygen. Enhanced proliferation and clonogenicity were also seen in p53-deficient transformed cells, suggesting that there is a substantial p53-independent component to oxidative-stress growth suppression. In addition, within an organism, tissue oxygenation occurs to lower partial pressures than atmospheric oxy-

high density (2 x 10^6 cells/plate)
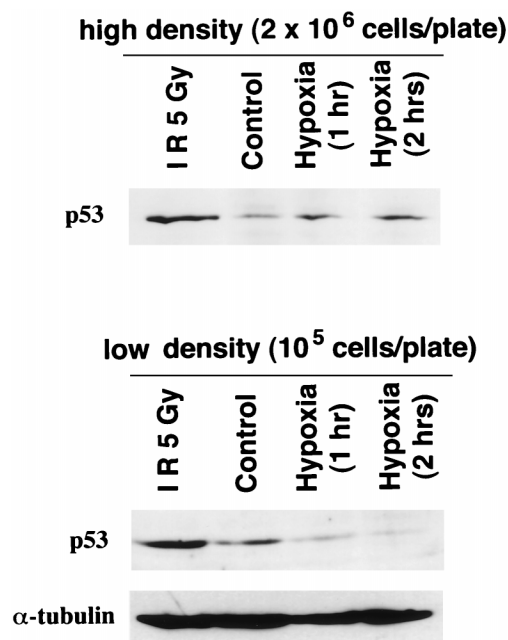

low density (10^5 cells/plate)

FIG. 7. p53 protein levels rise following hypoxia at high density (with acidosis), but fall following hypoxia at low density (without acidosis). p53 protein levels were determined by immunoblotting of lysates from cells exposed to hypoxia for the times indicated at 2×10^6 or 1×10^5 cells/60-mm-diameter dish and compared to those for oxic controls and cells treated with 5 Gy of ionizing radiation (IR) (measurements were made 2 h after irradiation). p53 levels rise at 2×10^6 cells/60-mm-diameter dish, although these cells eventually lose viability, whereas p53 levels fall at the low density (in the absence of acidosis), although these cells display enhanced viability (Fig. 6). Antitubulin (α-tubulin) reblotting (loading control) is shown for the low-density blot.

gen, so the beneficial effect seen in nonacidotic hypoxic cells is best considered to represent maintenance of cell cycle progression rather than an increase in S phase compared to that with atmospheric oxygen. It may also be important to consider cell type differences in these behaviors, which could vary between fibroblasts, epithelial cells, and hematopoietic cells, etc.

Hypoxia without acidosis. These studies demonstrate that transformation with specific oncogenes overrides the hypoxic cell cycle checkpoint in hypoxic fibroblasts in the absence of secondary acidosis. Oxygen has long been known to enhance the damaging effect of ionizing radiation, presumably by fixing the free radicals generated by radiation in the form of organic peroxides (22). H_2O_2 has been shown to induce apoptosis that could be prevented by Trolox, an antioxidant (15). Bcl-2, a major inhibitor of apoptosis, has been shown to prevent the formation of reactive oxygen intermediates (ROI) (25, 27), and the production of ROI has been suggested as a common factor for many apoptosis-inducing agents, although Bcl-2 may be protective even in the absence of ROI (26, 49). Culture with 95% oxygen without any additional treatment induces apoptosis in T-lymphoma cell lines (38). The same study (38) also demonstrates apoptosis induced by hypoxia, further arguing against oxygen radicals being required mediators of apoptosis. In the present study, apoptosis also appears not to require oxygen, as it still occurs in acidotic transformed fibroblasts under hypoxic conditions.

Clinical implications. Given the observation that nonacidotic hypoxic tumor cells appear to have lost the G_0/G_1 hypoxic checkpoint, are conditions likely to exist in vivo wherein this behavior might be clinically relevant? Although hypoxic zones have been thought to correlate with acidotic regions in isch-

emic tumors or tissues, tumor angiogenesis as well as venous drainage is generally disordered to a degree which may not preclude zones in which acidosis and hypoxia are not coincident. In fact, a recent analysis has demonstrated frequent discordance between hypoxic and acidotic zones in solid tumors in vivo (23). Another situation that could contribute to discordance between hypoxia and acidosis involves transient hypoxia, which could occur in a region where the pH is normal. At the individual cell level, conditions of venous drainage and arteriolar oxygenation are unlikely to be perfectly matched. In these circumstances, individual cells or small clusters might undergo hypoxic growth until, having outgrown their venous drainage, they accumulate acidosis and a different (and partially overlapping) zone of cells displays such growth. In this manner, one might envisage a rolling population of tumor cells which harbors dangerous proliferative potential within hypoxic zones of a tumor where many antineoplastic therapies fail to reach or function. Finally, the present study examined only chronic hypoxia, whereas large regions of tumors in vivo are subject to patterns of acute hypoxia, reoxygenation, and rehypoxiation (29; for a review, see reference 7). These factors may significantly alter the balance of hypoxia and acidosis as well as major variables of radio- and chemotherapy sensitivity.

REFERENCES

1. **Acker, H., G. Holtermann, and J. Carlsson.** 1992. Influence of glucose on metabolism and growth of rat glioma cells in multicellular spheroid culture. Int. J. Cancer **52:**279–285.
2. **Barry, M. A., and A. Eastman.** 1992. Endonuclease activation during apoptosis: the role of cytosolic Ca 2+ and pH. Biochem. Biophys. Res. Commun. **186:**782–789.
3. **Barry, M. A., and A. Eastman.** 1993. Identification of deoxyribonuclease II as an endonuclease involved in apoptosis. Arch. Biochem. Biophys. **300:**440–450.
4. **Barry, M. A., J. E. Reynolds, and A. Eastman.** 1993. Etoposide-induced apoptosis in human HL-60 cells is associated with intracellular acidification. Cancer Res. **53:**2349–2347.
5. **Bissell, M. J., C. Hatie, and H. Rubin.** 1972. Patterns of glucose metabolism in normal and virus-transformed chick cells in tissue culture. J. Natl. Cancer Inst. **49:**555–565.
6. **Brizel, D. M., S. P. Scully, J. M. Harrelson, L. J. Layfield, J. M. Bean, L. R. Prosnitz, and M. W. Dewhirst.** 1996. Tumor oxygenation predicts for the likelihood of distant metastases in human soft tissue sarcoma. Cancer Res. **56:**941–943.
7. **Brown, J. M., and A. J. Giaccia.** 1994. Tumour hypoxia: the picture has changed in the 1990s. Int. J. Radiat. Biol. **65:**95–102.
8. **Dewhirst, M. W., E. T. Ong, G. L. Rosner, S. W. E. Rehmus, S. Shan, R. D. Braun, D. M. Brizel, and T. W. Secomb.** 1996. Arteriolar oxygenation in tumor and subcutaneous arterioles: effects of inspired air oxygen content. Br. J. Cancer **74:**247–251.
9. **Dolbeare, F., and J. R. Selden.** 1994. Immunochemical quantification of bromodeoxyuridine: application to cell cycle kinetics, p. 298–316. *In* Z. Darzynkiewicz, J. P. Robinson, and H. A. Crissman (ed.), Flow cytometry, 2nd ed, vol. A. Academic Press, San Diego, Calif.
10. **Dyson, J. E. D., D. M. Simmons, J. Daniel, J. M. McLaughlin, P. Quirke, and C. C. Bird.** 1986. Kinetic and physical studies of cell death induced by chemotherapeutic agents or hyperthermia. Cell Tissue Kinet. **19:**311–324.
11. **Evan, G. I., A. H. Wyllie, C. S. Gilbert, T. D. Littlewood, H. Land, M. Brooks, C. M. Waters, L. Z. Penn, and D. C. Hancock.** 1992. Induction of apoptosis in fibroblasts by c-myc protein. Cell **69:**119–128.
12. **Fadock, V. M., D. R. Voelker, P. A. Campbell, J. J. Cohen, D. L. Bratton, and P. M. Henson.** 1992. Exposure of phosphatidylserine on the surface of apo-

ptotic lymphocytes triggers specific recognition and removal by macrophages. J. Immunol. **148:**2207–2216.

13. **Fandrey, J.** 1995. Hypoxia-inducible gene expression. Respir. Physiol. **101:** 1–10.

14. **Fisher, D. E.** 1994. Apoptosis in cancer therapy: crossing the threshold. Cell **78:**539–542.

15. **Forrest, V. J., Y.-H. Kang, D. E. McClain, D. H. Robinson, and N. Ramakrishnan.** 1994. Oxidative stress-induced apoptosis prevented by trolox. Free Radical Biol. Med. **16:**675–684.

16. **Gatenby, R. A., H. B. Kessler, J. S. Rosenblum, L. R. Coia, P. J. Moldofsky, W. H. Hartz, and G. J. Broder.** 1988. Oxygen distribution in squamous cell carcinoma metastases and its relationship to outcome of radiation therapy. Int. J. Radiat. Oncol. Biol. Phys. **14:**831–838.

17. **Gottlieb, R. A., H. A. Giesing, J. Y. Zhu, R. L. Engler, and B. M. Babior.** 1995. Cell acidification in apoptosis: granulocyte colony-stimulating factor delays programmed cell death in neutrophils by up-regulating the vacuolar H(+)-ATPase. Proc. Natl. Acad. Sci. **92:**5965–5968.

18. **Gottlieb, R. A., J. Nordberg, E. Skowronski, and B. M. Babior.** 1996. Apoptosis induced in Jurkat cells by several agents is preceded by intracellular acidification. Proc. Natl. Acad. Sci. USA **93:**654–658.

19. **Graeber, T. G., C. Osmanian, T. Jacks, D. E. Houseman, C. J. Koch, S. W. Lowe, and A. J. Giaccia.** 1996. Hypoxia-mediated selection of cells with diminished apoptotic potential in solid tumours. Nature **379:**88–91.

20. **Graeber, T. G., J. F. Peterson, M. Tsai, K. Monica, A. J. Fornace, Jr., and A. J. Giaccia.** 1994. Hypoxia induces accumulation of p53 protein, but activation of a G_1-phase checkpoint by low-oxygen conditions is independent of p53 status. Mol. Cell. Biol. **14:**6264–6277.

21. **Guillemin, K., and M. A. Krasnow.** 1997. The hypoxic response: huffing and HIFing. Cell **89:**9–12.

22. **Hall, E. J.** 1994. The oxygen effect and reoxygenation, p. 133–152. *In* E. J. Hall (ed.), Radiobiology for the radiologist, 4th ed. J.B. Lippincott, Philadelphia, Pa.

23. **Helmlinger, G., F. Yuan, M. Dellian, and R. K. Jain.** 1997. Interstitial pH and pO_2 gradients in solid tumors in vivo: high-resolution measurements reveal a lack of correlation. Nat. Med. **3:**177–182.

24. **Herrmann, M., N.-M. Lorenz, R. Voll, M. Grunke, W. Worth, and J. R. Kalden.** 1994. A rapid and simple method for the isolation of apoptotic DNA fragments. Nucleic Acids Res. **22:**5506–5507.

25. **Hockenbery, D. M., Z. N. Oltvai, X.-M. Yin, C. L. Milliman, and S. J. Korsmeyer.** 1993. Bcl-2 functions in an antioxidant pathway to prevent apoptosis. Cell **75:**241–251.

26. **Jacobson, M. D., and M. C. Raff.** 1995. Programmed cell death and Bcl-2 protection in very low oxygen. Nature **374:**814–816.

27. **Kane, D. J., T. A. Safafian, R. Anton, H. Hahn, E. B. Gralla, J. S. Valentine, T. Ord, and D. E. Bredesen.** 1993. Bcl-2 inhibition of neural death: decreased generation of reactive oxygen species. Science **262:**1274–1277.

28. **Kaufmann, S. H., S. Desnoyers, Y. Ottaviano, N. E. Davidson, and G. G. Poirier.** 1993. Specific proteolytic cleavage of poly(ADP-ribose) polymerase: an early marker of chemotherapy induced apoptosis. Cancer Res. **53:**3976–3985.

29. **Kimura, H., R. D. Braun, E. T. Ong, R. Hsu, T. W. Secomb, D. Papahadjopoulos, K. Hong, and M. W. Dewhirst.** 1996. Fluctuations in red cell flux in tumor microvessels can lead to transient hypoxia and reoxygenation in tumor parenchyma. Cancer Res. **56:**5522–5528.

30. **Koch, C. J.** 1984. A thin-film culturing technique allowing rapid gas-liquid equilibration (6 sec) with no toxicity to mammalian cells. Radiat. Res. **97:** 434–442.

31. **Koch, C. J., and J. Kruuv.** 1972. Correspondence. Br. J. Radiol. **45:**788.

32. **Koh, W.-J., J. S. Rasey, M. L. Evans, J. R. Grierson, T. K. Lewellen, M. M. Graham, K. A. Krohn, and T. W. Griffin.** 1992. Imaging of hypoxia in human tumors and [F18] fluormisonidazole. Int. J. Radiat. Oncol. Biol. Phys. **22:** 199–212.

33. **Lazebnik, Y. A., S. H. Kaufmann, S. Desnoyers, G. G. Poirier, and W. C. Earnshaw.** 1994. Cleavage of poly(ADP-ribose) polymerase by a proteinase with properties like ICE. Nature **371:**346–347.

34. **Lowe, S. W., T. Jacks, D. E. Houseman, and H. E. Ruley.** 1994. Abrogation of oncogene-associated apoptosis allows transformation of p53-deficient cells. Proc. Natl. Acad. Sci. USA **91:**2026–2030.

35. **Morana, S. J., C. M. Wolf, J. Li, J. E. Reynolds, M. D. Brown, and A. J. Eastman.** 1996. The involvement of protein phosphatases in the activation of ICE/CED-3 protease, intracellular acidification. DNA digestion, and apoptosis. J. Biol. Chem. **271:**18263–18271.

36. **Morrow, C. S., and K. H. Cowan.** 1993. Mechanisms of antineoplastic resistance, p. 340–348. *In* D. T. DeVita, S. Hellman, and S. A. Rosenberg (ed.), Cancer, principles and practice of oncology, 4th ed., vol. 1. J.B. Lippincott, Philadelphia, Pa.

37. **Moulder, J. E., and S. Rowckwell.** 1984. Hypoxic fractions of solid tumors: experimental techniques, methods of analysis, and a survey of existing data. Int. J. Radiat. Oncol. Biol. Phys. **10:**695–712.

38. **Muschel, R. J., E. J. Bernhard, L. Garza, W. G. McKenna, and C. J. Koch.** 1995. Induction of apoptosis at different oxygen tensions: evidence that oxygen radicals do not mediate apoptotic signaling. Cancer Res. **55:**995–998.

39. **Nelson, W. G., and M. B. Kastan.** 1994. DNA strand breaks: the DNA template alterations that trigger p53-dependent DNA damage response pathways. Mol. Cell. Biol. **14:**1815–1823.

40. **Nicholson, D. W., A. All, N. A. Thornberry, J. P. Vaillancourt, D. C. K., M. Gallant, Y. Gareau, P. R. Griffin, M. Labelle, Y. A. Lazebnik, N. A. Munday, S. M. Raju, M. E. Smulson, T.-T. Yamin, V. L. Yu, and D. K. Miller.** 1995. Identification and inhibition of the ICE/CED-3 protease necessary for mammalian apoptosis. Nature **376:**37–43.

41. **Perez-Sala, D., D. Collado-Escobar, and F. Mollinedo.** 1995. Intracellular alkalinization suppresses lovastatin-induced apoptosis in HL-60 cells through the inactivation of a pH-dependent endonuclease. J. Biol. Chem. **270:**6235–6242.

42. **Rebollo, A., J. Gomez, A. Martinez de Aragon, P. Lastres, A. Silva, and D. Perez-Sala.** 1995. Apoptosis induced by IL-2 withdrawal is associated with an intracellular acidification. Exp. Cell Res. **218:**581–585.

43. **Reynolds, J. E., J. Li, R. W. Craig, and A. Eastman.** 1996. Bcl-2 and Mcl-1 expression in Chinese hamster ovary cells inhibits intracellular acidification and apoptosis induced by staurosporine. Exp. Cell Res. **225:**430–436.

44. **Sandford, K., and B. B. Westfall.** 1969. Growth and glucose metabolism of high and low tumor-producing clones under aerobic and anaerobic conditions in vitro. J. Natl. Cancer Inst. **42:**953–959.

45. **Schwickert, G., S. Walenta, K. Sundfor, E. K. Rofstad, and W. Mueller-Klieser.** 1995. Correlation of high lactate levels in human cervical cancer with incidence of metastasis. Cancer Res. **55:**4757–4759.

46. **Secomb, T. W., R. Hsu, M. W. Dewhirst, B. Klitzmann, and J. F. Gross.** 1993. Analysis of oxygen transport to tumor tissue by microvascular networks. Int. J. Radiat. Oncol. Biol. Phys. **25:**481–489.

47. **Secomb, T. W., R. Hsu, E. T. Ong, J. F. Gross, and M. W. Dewhirst.** 1995. Analysis of the effects of oxygen supply and demand on hypoxic fraction in tumors. Acta Oncol. **34:**313–316.

48. **Seymour, C. B., and C. Mothersill.** 1981. The effect of lactate on the radiation response of CHO-K1 cells in culture. Int. J. Radiat. Biol. **40:**283–291.

49. **Shimizu, S., Y. Eguchi, H. Kosaka, W. Kamiike, H. Matsuda, and Y. Tsujimoto.** 1995. Prevention of hypoxia-induced cell death by Bcl-2 and Bcl-xL. Nature **374:**811–813.

50. **Shrieve, D. C., D. F. Deen, and J. W. Harris.** 1983. Effects of extreme hypoxia on the growth and viability of EMT6/SF mouse tumor cells *in vitro*. Cancer Res. **43:**3521–3527.

51. **Takano, Y. S., B. V. Harmon, and J. F. R. Kerr.** 1991. Apoptosis induced by mild hyperthermia in human and murine tumor cell lines: a study using electron microscopy and DNA gel electrophoresis. J. Pathol. **163:**329–336.

52. **Teicher, B. A.** 1994. Hypoxia and drug resistance. Cancer Metas. Rev. **13:** 139–168.

53. **Teicher, B. A., J. S. Lazo, and A. C. Sartorelli.** 1981. Classification of antineoplastic agents by their selective toxicities toward oxygenated and hypoxic tumor cells. Cancer Res. **41:**73–81.

54. **Vaupel, P., K. Schlenger, C. Knoop, and M. Hockel.** 1991. Oxygenation of human tumors: evaluation of tissue oxygen distribution in breast cancers by computerized O_2 tension measurements. Cancer Res. **51:**3316–3322.

55. **Wahl, A. F., K. L. Donaldson, C. Fairchild, F. Y. Lee, S. A. Foster, G. W. Demers, and D. A. Galloway.** 1996. Loss of normal p53 function confers sensitization to Taxol by increasing G2/M arrest and apoptosis. Nat. Med. **2:** 72–79.

56. **Wike-Hooley, J. L., J. Haveman, and H. S. Reinhold.** 1984. The relevance of tumour pH to the treatment of malignant disease. Radiother. Oncol. **2:** 343–366.

57. **Woods, C. M., J. Zhu, P. A. McQueney, D. Bollag, and E. Lazarides.** 1995. Taxol-induced mitotic block triggers rapid onset of a p53-independent apoptotic pathway. Mol. Med. **1:**506–526.

58. **Yao, K.-S., M. Clayton, and P. J. O'Dwyer.** 1995. Apoptosis in human adenocarcinoma HT29 cells induced by exposure to hypoxia. J. Natl. Cancer Inst. **87:**117–122.